

NRC Publications Archive Archives des publications du CNRC

Laser Coulomb-explosion imaging of small molecules

Légaré, F.; Lee, Kevin; Litvinyuk, I.; Dooley, P.; Wesolowski, S.S.; Bunker, Philip; Dombi, P.; Krausz, F.; Bandrauk, A.D.; Villeneuve, D.; Corkum, P.B.

This publication could be one of several versions: author's original, accepted manuscript or the publisher's version. / La version de cette publication peut être l'une des suivantes : la version prépublication de l'auteur, la version acceptée du manuscrit ou la version de l'éditeur.

For the publisher's version, please access the DOI link below. / Pour consulter la version de l'éditeur, utilisez le lien DOI ci-dessous.

Publisher's version / Version de l'éditeur:

<https://doi.org/10.1103/PhysRevA.71.013415>

Physical Review. A, Atomic, Molecular, and Optical Physics, 71, 1, pp. 013415-1-013415-5, 2005-01-19

NRC Publications Archive Record / Notice des Archives des publications du CNRC :

<https://nrc-publications.canada.ca/eng/view/object/?id=7320bcc5-83fb-4b3e-ae16-50976d0f02a9>

<https://publications-cnrc.canada.ca/fra/voir/objet/?id=7320bcc5-83fb-4b3e-ae16-50976d0f02a9>

Access and use of this website and the material on it are subject to the Terms and Conditions set forth at

<https://nrc-publications.canada.ca/eng/copyright>

READ THESE TERMS AND CONDITIONS CAREFULLY BEFORE USING THIS WEBSITE.

L'accès à ce site Web et l'utilisation de son contenu sont assujettis aux conditions présentées dans le site

<https://publications-cnrc.canada.ca/fra/droits>

LISEZ CES CONDITIONS ATTENTIVEMENT AVANT D'UTILISER CE SITE WEB.

Questions? Contact the NRC Publications Archive team at

PublicationsArchive-ArchivesPublications@nrc-cnrc.gc.ca. If you wish to email the authors directly, please see the first page of the publication for their contact information.

Vous avez des questions? Nous pouvons vous aider. Pour communiquer directement avec un auteur, consultez la première page de la revue dans laquelle son article a été publié afin de trouver ses coordonnées. Si vous n'arrivez pas à les repérer, communiquez avec nous à PublicationsArchive-ArchivesPublications@nrc-cnrc.gc.ca.

Laser Coulomb-explosion imaging of small molecules

F. Légaré,^{1,2} Kevin F. Lee,^{1,3} I. V. Litvinyuk,⁴ P. W. Dooley,^{1,3} S. S. Wesolowski,¹ P. R. Bunker,¹ P. Dombi,⁵ F. Krausz,⁵
A. D. Bandrauk,² D. M. Villeneuve,¹ and P. B. Corkum¹

¹National Research Council of Canada, 100 Sussex Drive, Ottawa, Ontario, Canada K1A 0R6

²Département de Chimie, Université de Sherbrooke, Sherbrooke, Québec, Canada J1K 2R1

³Department of Physics & Astronomy, McMaster University, Hamilton, Ontario, Canada L8S 4M1

⁴Department of Physics, Kansas State University, Manhattan, Kansas 66506, USA

⁵Technische Universität Wien, Vienna, Austria

(Received 11 August 2004; published 19 January 2005)

We use intense few-cycle laser pulses to ionize molecules to the point of Coulomb explosion. We use Coulomb's law or *ab initio* potentials to reconstruct the molecular structure of D₂O and SO₂ from the correlated momenta of exploded fragments. For D₂O, a light and fast system, we observed about 0.3 Å and 15° deviation from the known bond length and bond angle. By simulating the Coulomb explosion for equilibrium geometry, we showed that this deviation is mainly caused by ion motion during ionization. Measuring three-dimensional structure with half bond length resolution is sufficient to observe large-scale rearrangements of small molecules such as isomerization processes.

DOI: 10.1103/PhysRevA.71.013415

PACS number(s): 33.80.Wz, 34.50.Gb, 42.50.Hz

Coulomb-explosion imaging was first demonstrated using small molecular ions moving with $\sim 10^6$ eV energies passing through a thin foil [1]. All ionization occurred within ~ 100 as. The initial structure is reconstructed by measuring the momentum of all fragments after explosion caused by multiple ionization. The reconstruction relies on knowledge of the potential that describes the interaction of the charged particles during the explosion. For simplicity, a Coulomb potential is typically used. This technique can measure the stationary states of small molecules relatively accurately, but is difficult to adapt to dynamic imaging. Lasers are being studied as an alternative to collision ionization because of their greater flexibility for pump-probe experiments [2].

Exploiting the recent development of intense, few-cycle laser pulses [3], we investigate their interaction with small molecules. Even with 5 fs optical pulses, laser ionization will be about 50 times slower than collision. This will make the image less accurate. The question is, how well can we freeze nuclear position during rapid ionization induced with state-of-the-art laser technology? To answer this question, we measured the three-dimensional structures of both D₂O and SO₂ by Coulomb-explosion imaging with a few-cycle laser pulse and compared them to the known structures. We simulate the Coulomb explosion of D₂O by using an atomic tunneling model to describe ionization, and classical mechanics to describe the motion of the fragments. We show that motion occurs during ionization but the image is sufficiently accurate to resolve changes on the length scale of a chemical bond. In comparison to heavy water, our SO₂ images are even closer to the known ground stationary state geometry due to better confinement of the heavier nuclei.

Laser-driven Coulomb explosion has already been extensively investigated [4,5]. In most experiments reported so far, the time scale of ionization was comparable with the time scale of molecular dynamics (10–100 fs). When ionization and dissociation occur simultaneously, dissociation occurs on the field-distorted potential energy surfaces of a succession of charge states, making it very complex. With ~ 50 fs pulses, accurate imaging was only possible for heavy mol-

ecules [2] such as iodine. By using few-cycle laser pulses we remove much of this complexity.

Numerical simulations of laser Coulomb explosion of H₂⁺ [6] and experiments with D₂ [7] were the only previous studies of the interaction of intense few-cycle laser pulses with molecules. Both suggest the possibility of using intense few-cycle laser pulses as an imaging technique in dynamics experiments. We extend this work to small polyatomic molecules.

We compress the 40 fs pulses from a Ti:sapphire (800 nm, ~ 500 μ J, 500 Hz) regenerative amplifier using self-phase modulation in an argon-filled hollow core fiber followed by dispersion compensation with chirped mirrors. We characterized the pulses using SPIDER [8]. We produced 7 fs pulses but over the duration of the experiment the pulse duration may have increased to ~ 8 fs due to laser fluctuations. A low density, ~ 40 - μ m-thick molecular beam propagated perpendicular to the 24-cm-long imaging-time-of-flight spectrometer axis [9]. The laser was focused ($f=50$ mm) perpendicular to both the molecular beam and the spectrometer axis inside a vacuum chamber (10^{-9} mbar background pressure). The tight focus ensured that our interaction volume was small (1000 μ m³) compared to the time-of-flight dimension. Errors due to the size of the interaction volume were negligible.

Our position- and time-sensitive multiple-hit ion detector can measure the velocity vectors of up to 16 fragments per laser pulse. As the beam density was low ($<10^{11}$ cm⁻³), an average of less than one molecule was exploded per laser shot. For a single molecule explosion event, momentum conservation requires that the total momentum is zero. To verify that only triply coincident ions were recorded, we required that the total momentum of all three particles was less than 5×10^{-23} kg m/s. We estimate a false coincidence rate of about 3%.

Figure 1 compares D₂O⁴⁺ explosion ($\rightarrow D^+ + O^{2+} + D^+$) with 8 fs ($\sim 5 \times 10^{15}$ W/cm²) and 40 fs ($\sim 3 \times 10^{15}$ W/cm²) linearly polarized laser pulses. While charge

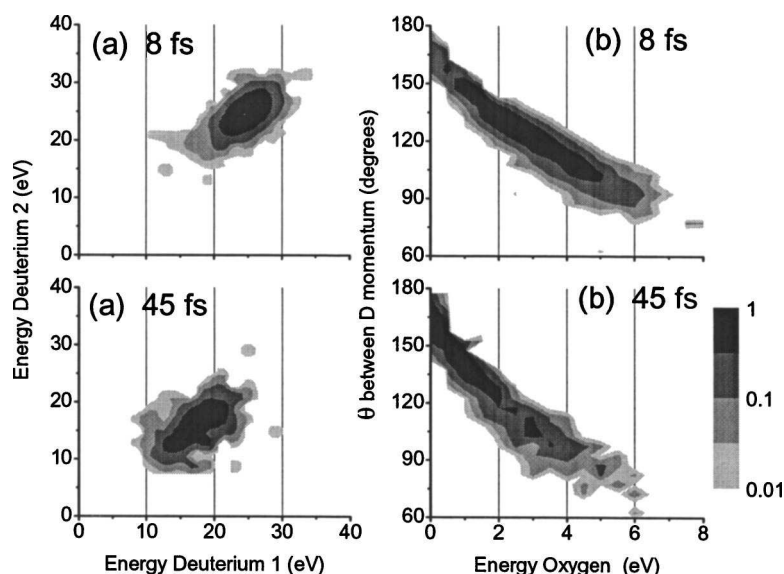


FIG. 1. Comparison of D_2O^{4+} explosion ($\rightarrow \text{D}^+ + \text{O}^{2+} + \text{D}^+$) between an 8 and 40 fs laser pulse. (a) Energy-energy correlation for D^+ . (b) Angle between D^+ momenta.

states up to $5+$ were observed, we selected the D_2O^{4+} channel because of its higher count rate. Lower charge states give lower total kinetic energy. Using a modified Ammosov-Delone-Krainov (ADK) theory [10], at $5 \times 10^{15} \text{ W/cm}^2$, we estimated respective ionization rates of 10^{16} and 10^{14} s^{-1} for the $\text{D}_2\text{O}^{2+} \rightarrow \text{D}_2\text{O}^{3+}$ and $\text{D}_2\text{O}^{3+} \rightarrow \text{D}_2\text{O}^{4+}$ charge state transitions.

Instantaneous ionization of ground state D_2O at its equilibrium position to the electronic ground state D_2O^{4+} yields a total fragment kinetic energy of $\sim 65 \text{ eV}$. The partition of energy leaves D^+ with 31 eV and O^{2+} with 3 eV . The angle between the momentum vectors of D^+ is 128° . In Fig. 1(a), we observe that both D^+ from the same molecule have similar kinetic energy since the distribution lies on the diagonal of the energy-energy correlation map. For 8 fs laser pulses, the results of Figs. 1(a) and 1(b) are much closer to the expected value than they would be with 40 fs pulses. For 8 fs pulses, the D^+ energy peaks at 24 eV , the O^{2+} energy peaks at 2.3 eV , the angle between vectors peaks at 123° , and the total kinetic energy distribution peaks at 53 eV compared to 35 eV with 40 fs laser pulses.

The correlation map for 40 fs shown in Fig. 1 is characteristic of enhanced ionization [11,12]. It does not change as the pulse duration is increased to 100 fs (or more). Coulomb-explosion imaging is not as useful in the enhanced ionization regime, since the fragmentation is almost independent of the internal structure. The near absence of enhanced ionization from the 8 fs kinetic energy distribution is consistent with D_2 results [7].

For each event that makes up Fig. 1, the vector momentum of each ion was measured. The inferred atomic positions are directly related to the fragment momentum distribution. However, obtaining a mathematical transformation connecting the correlated velocities with the positions of the atoms for polyatomic molecules is difficult, and remains a subject of current research [13]. Our iterative procedure for reconstructing molecular structure assumes classical motion on an *ab initio* or Coulombic potential with zero initial velocity. For each event in the correlated momentum distribution, we find a three-dimensional structure that reproduces the mea-

sured fragment velocities. We estimate experimental error due to detector precision (time of flight and detector position) to be about 5° and 0.02 \AA for each individual structure. The term “Coulomb explosion” implies that the Coulomb potential adequately approximates the true potential energy surface of the exploding ion when the charge state is high. We confirm the validity of this approximation by comparison with the *ab initio* potential for D_2O^{4+} .

The *ab initio* calculation of the potential energy surface of the D_2O^{4+} molecular ion was carried out for 38 geometries covering bond angles from 90° to 180° , and bond lengths from 0.85 to 2.0 \AA . Energies were computed using an augmented correlation-consistent polarized-valence quadruple-zeta (aug-cc-pVQZ) basis set [14]. Reference electronic wave functions were obtained using the spin-restricted Hartree-Fock (RHF) method, and dynamical correlation was incorporated using the coupled-cluster method including all single and double excitations as well as a perturbative estimate of connected triple excitations [CCSD(T)] [15]. During the correlation procedure, the oxygen $1s$ core electrons were held frozen.

Figure 2(a) shows a set of structures obtained using 8 fs pulses and the *ab initio* potential. Figures 2(b) and 2(c) show the bond length (R_{OD}) and the bond angle (θ_{DOD}) distributions for the structures shown in Fig. 2(a). For the stationary state geometry of D_2O , $R_{\text{OD}} = 0.96 \text{ \AA}$ and $\theta_{\text{DOD}} = 104.5^\circ$. When fitted to a Gaussian, our radial distribution R_{OD} peaks at 1.24 \AA [with a 0.3 \AA full width at half maximum (FWHM)] and θ_{DOD} peaks at 117° (58° FWHM). Using the Coulomb potential for reconstruction, R_{OD} peaks at 1.26 \AA and $\theta_{\text{DOD}} = 117^\circ$. The *ab initio* and Coulomb potentials yield nearly identical results for 8 fs laser pulses. In Figs. 2(b) and 2(c), the dotted curves represent the distributions for the ground stationary state structure of D_2O . For the radial distribution, results similar to D_2 [7] are seen. We observe no dependence of the measured structure on the orientation of the molecule with respect to the polarization axis. We address the substantial broadening of the bond angle distribution below.

The error introduced by the finite duration of the laser

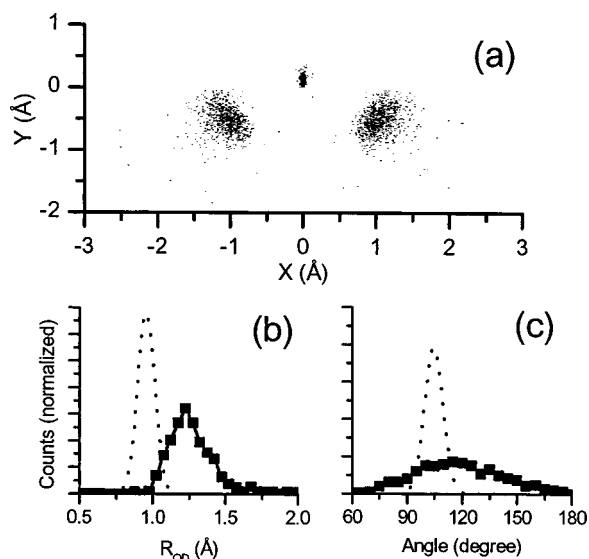


FIG. 2. (a) Structure of D_2O using the $4+$ charge states ($D_2O^{4+} \rightarrow D^+ + O^{2+} + D^+$). The reconstruction is achieved by using an *ab initio* potential. The center of mass is at $x=0$, $y=0$, and the y axis is the bisector of the angle. (b) Radial distribution. (c) Angular distribution. In (b) and (c), the dotted curve represents what we should expect for the $v=0$ stationary state structure of D_2O .

pulse can greatly exceed that of the approximate Coulomb potential. For instance, we found that imaging with 40 fs pulses yielded values of $R_{OD}=1.96 \text{ \AA}$ (0.9 \AA FWHM) and $\theta_{DOD}=138^\circ$ (75° FWHM). These results are consistent with those obtained by Sanderson *et al.* [5]. As in earlier D_2 experiments [10], a few-cycle laser pulse clearly improves our ability to measure molecular structure. Nevertheless, discrepancies remain. For D_2 , the measured kinetic energy distribution differed from that expected for an ideal Coulomb explosion because of motion on the intermediate charge states between the time of the first and final ionization and because the ionization potential depends on the internuclear separation. With 8 fs laser pulses, the former effect is more important.

We estimated the role of intermediate charge state dynamics for D_2O by simulating dissociative ionization. We assumed an 8 fs FWHM Gaussian pulse with a peak intensity of $5 \times 10^{15} \text{ W/cm}^2$. We described ionization using a tunneling model [10] and followed the nuclear motion by solving the classical equations of motion on the ground state ionic potential. We began with D_2O at rest in its stationary state geometry. We further assumed that the width of R_{OD} in Fig. 2(b) is primarily due to ionization dynamics rather than the size of the initial D_2O vibrational wave function. We simulated nuclear motion on the ground state potential surfaces of each charge state, tracking the probability of ionization as the nuclei moved. When the probability of ionization exceeded a random number ($0 < P_{\text{ionization}} \leq 1$), a transition to the next charge state was made. A distribution of nuclear positions was predicted by running 1000 trajectories. Once four electrons were removed, no further ionization was allowed. In this manner, we obtained a total kinetic energy of $\sim 55 \text{ eV}$ after the explosion, with an average R_{OD} of $\sim 1.38 \text{ \AA}$ and θ_{DOD} of $\sim 114^\circ$.

The D_2O simulation gives similar but not identical structure to the one reconstructed from the experimental results. The main reason for this difference is that by the time D_2O^{4+} was reached, the ions had accumulated $\sim 3\text{--}4 \text{ eV}$ of kinetic energy, while our reconstruction assumed initial fragment velocities of zero. In conjunction with our structure retrieval algorithm, the simulated asymptotic fragment velocity distribution yielded values of $R_{OD}=1.18 \text{ \AA}$ and $\theta_{DOD}=127^\circ$. While the simulated and experimental values are similar, the zero-initial-velocity assumption gives rise to discrepancies of $\sim 0.2 \text{ \AA}$ for the bond length and $\sim 15^\circ$ for the bond angle.

Our model shows that the deviation of R_{OD} from its known value is primarily due to motion on the ground state surfaces of intermediate molecular ions. However, ground state motion cannot account for the width of the θ_{DOD} distribution. We repeated the simulation using the first excited electronic state of D_2O^+ rather than the ground electronic state. The energy difference between these two states is $\sim 2 \text{ eV}$, which is about the energy of one 800 nm photon. Since the potential minimum for the excited state corresponds to a linear molecular geometry, the apparent bond angle will increase with the amount of time the wave packet spends on this potential surface. Using this state for the D_2O^+ surface, we find that the bond length is $\sim 1.40 \text{ \AA}$ with $\theta_{DOD} \sim 129^\circ$ when D_2O^{4+} is reached. Thus, it appears that for 8 fs pulses, motion on the ground and excited states leads to relatively small ($\sim 0.4 \text{ \AA}$) errors in laser Coulomb-explosion imaging of D_2O . However, for the angle, we see a 15° difference between the ground and excited D_2O^+ results. We believe that the broadening of the angular distribution results from the contribution of several different electronic states to the dynamics. In Coulomb explosion induced by collision, such broadening has been observed and attributed to the contribution of several electronic states in the final charge state [16,17]. In our case, there is in addition to this effect the contribution of electronic states on intermediate charge states populated during the multiple ionization. To improve the image further, even shorter intense pulses are needed.

Recently, intense 4 fs laser pulses were produced using self-phase modulation with a two-stage hollow-core fiber configuration [3]. We have simulated Coulomb explosion of D_2O with a 4 fs FWHM Gaussian pulse, neglecting the possibility of Coulomb blockade [7]. The simulation predicts a measured bond length of $\sim 1.14 \text{ \AA}$ and an angle of $\sim 109^\circ$ (D_2O^+ ground state). While these better approximate the stationary state geometry, discrepancies remain due to nuclear motion (which can be very fast in high charge states) during ionization. Nuclear motion in ions is extremely fast, because of charge interaction. However, as the importance of this motion decreases, the dependence of the ionization rate on atomic positions becomes more important. In addition, for 4 fs pulses, the Coulomb approximation may be less applicable. Instantaneous transition from D_2O to D_2O^{4+} gives 65 eV if we use the *ab initio* potential versus 70 eV for the Coulombic one. For 8 fs pulses, the Coulomb and the *ab initio* potentials converge before the wave packet reaches the D_2O^{4+} state. Thus, we found no difference between the two potentials for molecular reconstruction in the 8 fs case.

We now turn our attention to a molecule with heavier nuclei: SO_2 . Like D_2O , SO_2 is bent. Figure 3(a) presents the

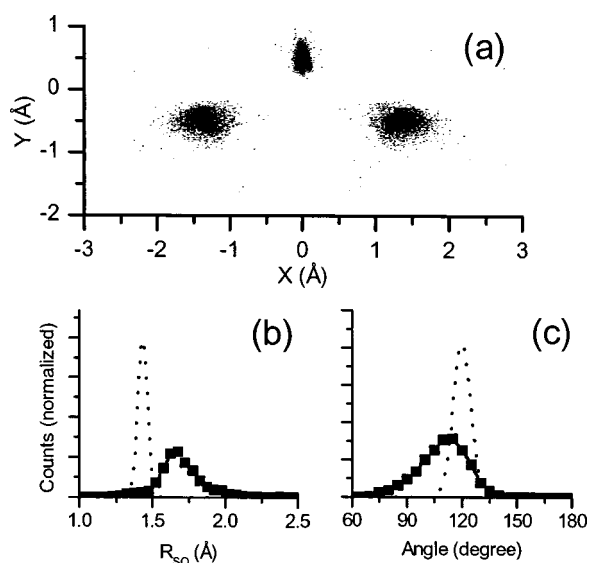


FIG. 3. (a) Structure of SO_2 using the SO_2^{7+} charge states ($\text{SO}_2^{7+} \rightarrow \text{O}^{2+} + \text{S}^{3+} + \text{O}^{2+}$). The reconstruction is achieved using the Coulombic potential. The center of mass is at $x=0$, $y=0$, and the y axis is the bisector of the angle. (b) Radial distribution. (c) Angular distribution. In (b) and (c), the dotted curve represents what we should expect for the $v=0$ stationary state structure of SO_2 .

distribution of SO_2 structures that we measured using the $7+$ charge state ($\text{SO}_2^{7+} \rightarrow \text{O}^{2+} + \text{S}^{3+} + \text{O}^{2+}$) produced using ~ 8 fs laser pulses. This is the highest charge we observed with reasonable count rate. In Figs. 3(b) and 3(c), we show the measured R_{SO} and θ_{OSO} distributions. The total fragment kinetic energy spectrum peaks at ~ 125 eV (not shown) whereas instantaneous Coulomb explosion would yield a value of ~ 145 eV. The expected stationary state geometry values for SO_2 are $R_{\text{SO}} = 1.43$ Å and $\theta_{\text{OSO}} = 119.5^\circ$. By assuming a Coulomb potential for the $7+$ charge state, we measured mean structural values of $R_{\text{SO}} = 1.67$ Å (0.26 Å FWHM) and $\theta_{\text{OSO}} = 111^\circ$ (30° FWHM). Using 50 fs laser pulses, Hishikawa *et al.* have reported a total fragment kinetic energy distribution peaking at 61.5 eV and values of $R_{\text{SO}} \sim 3.3$ Å and $\theta_{\text{OSO}} \sim 130^\circ$ [4]. Although molecules containing heavier nuclei might seem easier to image using laser-induced Coulomb explosion, this is not necessarily so. With heavier nuclei, more electrons must be removed to make the explosion Coulombic. The higher the charge state on which the nuclei move, the more the wave function will distort in a given amount of time due to stronger forces.

Unlike D_2O , we found that the measured SO_2 bond angle depends on the molecule's orientation with respect to the laser polarization axis. When the OO axis is parallel to the

polarization axis, the measured bond angle is 120° . When the axis of symmetry of SO_2 (C_{2v} axis) is parallel to the polarization, we measure a bond angle of 100° . The induced dipole and/or enhanced ionization [11,12] may be responsible for this distortion. Figure 3 contains the results for all orientations.

For both molecules, we observe that the ionization rate ($\text{D}_2\text{O} \rightarrow \text{D}_2\text{O}^{4+}$ and $\text{SO}_2 \rightarrow \text{SO}_2^{7+}$) is strongly dependent on the orientation of the molecules to the laser polarization. The favored orientation is when the OO axis (or DD) is parallel to the polarization axis (approximately one order of magnitude greater rate compared with molecules where the C_{2v} axis is parallel). For molecules whose plane is perpendicular to the polarization axis, the ionization rate is approximately two orders of magnitude lower than the favored axis. Angle-dependent ionization rates have been measured for diatomic molecules [18].

While laser Coulomb-explosion imaging technology is still improving, there appears to be a fundamental limit to image fidelity. The ionization rate of an atom or a molecule depends on its ionization potential, which varies as a function of the nuclear coordinates. This coordinate dependence will distort the measured probability density describing the nuclear wave function if the ionization rate is not saturated, irrespective of pulse duration. Thus, laser Coulomb-explosion imaging is less suitable for measuring stationary state molecular structures than spectroscopic or thin foil techniques [1]. However, the ultimate goal for laser Coulomb-explosion imaging is to follow structural changes during photochemical reactions.

We have shown that currently available laser pulses are capable of imaging the structures of small polyatomic molecules containing either heavy or light constituents with sub-bond-length resolution. Although we did not initiate and measure dynamics, it is feasible to do so. For example, imaging dramatic changes such as isomerization from *trans* to *cis* structures will be possible. Measurements of photochemically induced processes such as proton transfer reactions [19,20] will be particularly interesting. Laser-initiated Coulomb explosion could also be applied to structures of transition states that are highly transient and of great importance to chemistry.

The authors thank Professor Fritz Schaefer (University of Georgia) for providing computational resources for the *ab initio* calculations. The authors appreciate financial support from Canada's Natural Science and Engineering Research Council, NRC/CNRS collaborative research fund, the Canadian Institute for Photonics Innovation, and Le Fonds Québécois de la Recherche sur la Nature et les Technologies.

- [1] E. P. Kanter, P. J. Cooney, D. S. Gemmell, K.-O. Groeneveld, W. J. Pietsch, A. J. Ratkowski, Z. Vager, and B. J. Zabransky, *Phys. Rev. A* **20**, 834 (1979).
- [2] H. Stapelfeldt, H. Sakai, E. Constant, and P. B. Corkum, *Phys. Rev. A* **55**, R3319 (1997).

- [3] B. Schenkel, J. Biegert, U. Keller, C. Vozzi, M. Nisoli, G. Sansone, S. Stagira, S. De Silvestri, and O. Svelto, *Opt. Lett.* **28**, 1987 (2003).
- [4] A. Hishikawa, A. Iwamae, K. Hoshina, M. Kono, and K. Yamanouchi, *Chem. Phys. Lett.* **282**, 283 (1998).

- [5] J. H. Sanderson, A. El-Zein, W. A. Bryan, W. R. Newell, A. J. Langley, and P. F. Taday, *Phys. Rev. A* **59**, R2567 (1999).
- [6] S. Chelkowski, P. B. Corkum, and A. D. Bandrauk, *Phys. Rev. Lett.* **82**, 3416 (1999).
- [7] F. Légaré, I. V. Litvinyuk, P. W. Dooley, F. Quéré, A. D. Bandrauk, D. M. Villeneuve, and P. B. Corkum, *Phys. Rev. Lett.* **91**, 093002 (2003).
- [8] C. Iaconis and I. A. Walmsley, *Opt. Lett.* **23**, 792 (1998).
- [9] P. W. Dooley, I. V. Litvinyuk, Kevin F. Lee, D. M. Rayner, D. M. Villeneuve, and P. B. Corkum, *Phys. Rev. A* **68**, 023406 (2003).
- [10] G. L. Yudin and M. Yu Ivanov, *Phys. Rev. A* **64**, 013409 (2001).
- [11] T. Seideman, M. Yu Ivanov, and P. B. Corkum, *Phys. Rev. Lett.* **75**, 2819 (1995).
- [12] T. Zuo and A. D. Bandrauk, *Phys. Rev. A* **52**, R2511 (1995).
- [13] K. Nagaya and A. D. Bandrauk (private communication).
- [14] T. H. Dunning, *J. Chem. Phys.* **90**, 1007 (1989); R. A. Kendall, T. H. Dunning, and R. J. Harrison, *ibid.* **96**, 6796 (1992).
- [15] T. D. Crawford and H. F. Schaefer, *Rev. Comput. Chem.* **14**, 33 (2000), and references therein.
- [16] B. Siegmann, U. Werner, H. O. Lutz, and R. Mann, *J. Phys. B* **34**, L587 (2001).
- [17] D. Mathur, *Phys. Rep.* **391**, 1 (2004).
- [18] I. V. Litvinyuk, Kevin F. Lee, P. W. Dooley, D. M. Rayner, D. M. Villeneuve, and P. B. Corkum, *Phys. Rev. Lett.* **90**, 233003 (2003).
- [19] S. Nagaoka and U. Nagashima, *Chem. Phys.* **136**, 153 (1989).
- [20] T. Osipov, C. L. Cocke, M. H. Prior, A. Landers, Th. Weber, O. Jagutzi, L. Schmidt, H. Schmidt-Böcking, and R. Dörner, *Phys. Rev. Lett.* **90**, 233002 (2003).